THE JOURNAL OF BIOLOGICAL CHEMISTRY VOL. 284, NO. 28, pp. 18605–18613, July 10, 2009

Bacterial Toxin HigB Associates with Ribosomes and Mediates Translation-dependent mRNA Cleavage at A-rich Sites*[S]

Received for publication, March 5, 2009, and in revised form, April 15, 2009 Published, JBC Papers in Press, May 7, 2009, DOI 10.1074/jbc.M109.008763

Jennifer M. Hurley[1] **and Nancy A. Woychik**[2]

From the Department of Molecular Genetics, Microbiology and Immunology, University of Medicine and Dentistry of New Jersey-Robert Wood Johnson Medical School, Piscataway, New Jersey 08854

Most pathogenic *Proteus* species are primarily associated with urinary tract infections, especially in persons with indwelling catheters or functional/anatomic abnormalities of the urinary tract. Urinary tract infections caused by *Proteus vulgaris* typically form biofilms and are resistant to commonly used antibiotics. The Rts1 conjugative plasmid from a clinical isolate of *P. vulgaris* carries over 300 predicted open reading frames, including antibiotic resistance genes. The maintenance of the Rts1 plasmid is ensured in part by the HigBA toxin-antitoxin system. We determined the precise mechanism of action of the HigB toxin *in vivo*, which is distinct from other known toxins. We demonstrate that HigB is an endoribonuclease whose enzymatic activity is dependent on association with ribosomes through the 50 S subunit. Using primer extension analysis of several test mRNAs, we showed that HigB cleaved extensively across the entire length of coding regions only at specific recognition sequences. HigB mediated cleavage of 100% of both in-frame and out-of-frame AAA sequences. In addition, HigB cleaved ~20% of AA sequences in coding regions and occasionally cut single As. Remarkably, the cleavage specificity of HigB coincided with one of the most frequently used codons in the AT-rich *Proteus* spp., AAA (lysine). Therefore, the HigB-mediated plasmid maintenance system for the Rts1 plasmid highlights the intimate relationship between host cells and extrachromosomal DNA that enables the dynamic acquisition of genes that impart a spectrum of survival advantages, including those encoding multidrug resistance and virulence factors.

Toxin-antitoxin (TA)[3]/addiction/suicide modules typically include an autoregulated operon encoding a labile antitoxin and a more stable toxic protein (1). TA toxins facilitate stress survival (chromosomal) or plasmid maintenance and post-segregational killing (extrachromosomal; reviewed in Refs. 1, 2). Most chromosomal TA toxins inhibit cell growth by reversibly targeting either protein translation or DNA replication; their cognate antitoxins prevent toxin activity during periods of optimal growth but enable finely tuned control of TA module toxicity during relatively short periods of environmental stress. However, prolonged stress leads to a point of no return and cell death (3–5).

There are six confirmed chromosomal TA loci in *Escherichia coli* K12 cells: *dinJ-yafQ*, *relBE, yefM-yoeB, mazEF, chpBI-BK,* and *hipBA*. The toxins MazF and ChpBK are sequence-specific endoribonucleases that cleave free mRNA (6–10). The RelE toxin interacts with the ribosome and induces mRNA cleavage with a preference for the UAG stop codon (11–13). The YafQ toxin is a ribosome-associated endoribonuclease that cleaves in-frame AAA codons that are followed by either an A or G in the subsequent codon (14). The YoeB toxin inhibits translation at the initiation step, apparently by destabilization of the initiation complex (15). HipA toxin is a kinase whose mechanism of action is not known (16, 17).

Although the mechanism of action of many *E. coli* chromosomal and plasmid-derived toxins has been determined, the precise function of the HigB toxin has not been characterized. The *higBA* TA module is not present in *E. coli* K12; it resides on the Rts1 plasmid that typically replicates in *Proteus* spp. and imparts kanamycin resistance as well as temperature-sensitive post-segregational killing at 42 °C (18, 19). Interestingly, one or more chromosomal counterparts of *higBA* have been reported for several pathogens, including *Vibrio cholerae*, *Streptococcus pneumoniae, E. coli* CFT073, and *E. coli* O157:H7 (20). Some characterization of the two *V. cholerae* HigBA modules has been performed. First, one of the two *higBA* modules was shown to possess the general characteristics of TA systems by demonstration of toxin-antitoxin interaction, module organization/regulation, HigB toxicity, and rescue of toxicity with the cognate HigA antitoxin (21). Overexpression of HigB derived from two individual *higBA* modules encoded in *V. cholerae* or from Rts1 leads to inhibition of protein synthesis through translation-dependent mRNA cleavage in a manner similar to, but distinct from, RelE (22).

HigB is a member of the RelE family of toxins, including RelE, YafQ, and YoeB (20). In this study, we have identified the precise mode of action of HigB from Rts1. HigB associated with the 50 S ribosomal subunit, and this HigB-ribosome complex cleaved within mRNA coding regions at all AAA triplet sequences, both in-frame and out-of-frame. HigB appeared to be responsible for the mRNA cleavage activity of the HigB-

* This work was supported, in whole or in part, by National Institutes of Health Grants GM74097 and U54 Grant GM74958 (NE Structural Genomics Consortium). This work was also supported by Takara Bio, Inc.

[S] The on-line version of this article (available at http://www.jbc.org) contains supplemental Figs. 1 and 2.

[1] Supported by National Institutes of Health T32 Training Grant AI07403, Virus-Host Interactions in Eukaryotic Cells from the NIAID (awarded to S. Pestka).

[2] To whom correspondence should be addressed: UMDNJ-Robert Wood Johnson Medical School, Dept. of Molecular Genetics, Microbiology and Immunology, 675 Hoes La., Piscataway, NJ 08854-5635. Fax: 732-235-5223; E-mail: nancy.woychik@umdnj.edu.

[3] The abbreviations used are: TA, toxin-antitoxin; ORF, open reading frame.

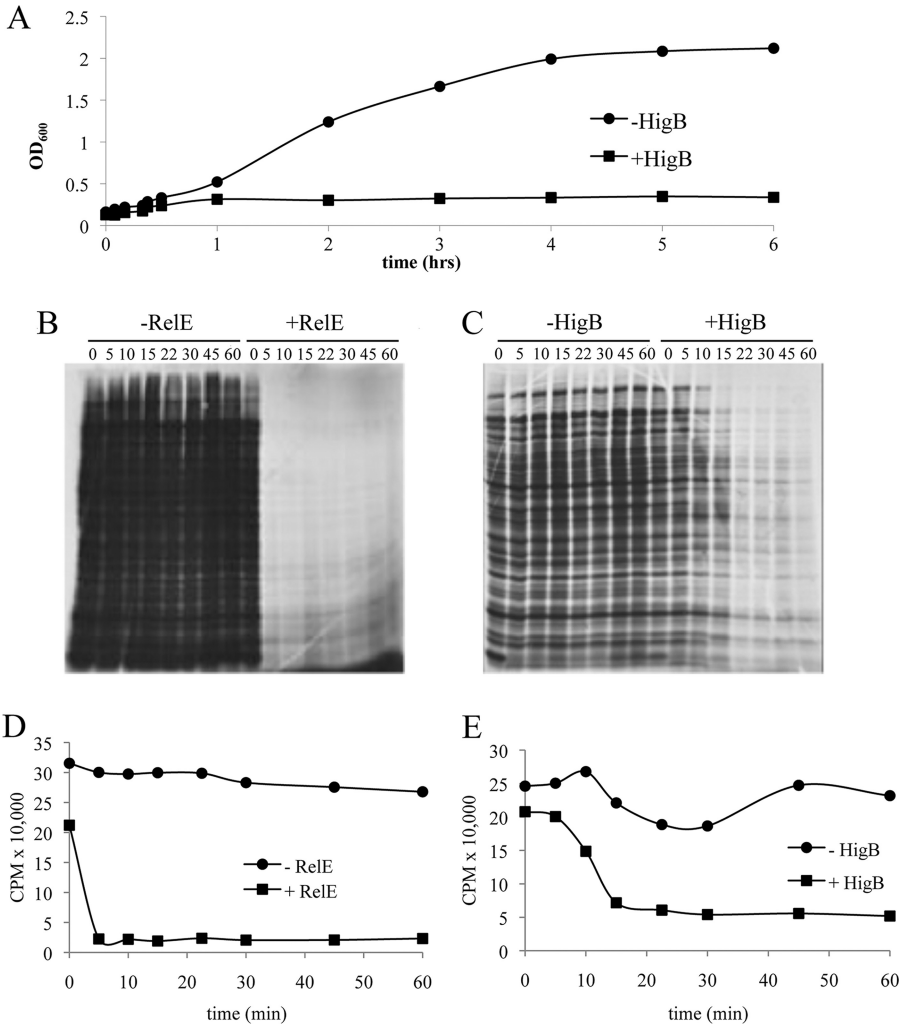

FIGURE 1. **Expression of HigB leads to translation arrest.** *A*, growth profile of HigB-induced (arabinose +) or uninduced (arabinose −) BW25113 cells containing pBAD24-*higB* grown at 37 °C in M9 medium containing either glucose (uninduced) or glycerol (induced). *B* and *C*, [^{35}S]methionine incorporation of RelE- or HigB-induced *versus* uninduced cells *in vivo*. Equivalent amounts of cell lysate, derived from equal culture volumes, were subjected to SDS-PAGE, followed by autoradiography. *D* and *E*, quantification of [^{35}S]methionine incorporation into RelE- or HigB-induced (arabinose +) or uninduced (arabinose −) cells. Counts/min were the result of trichloroacetic acid-precipitated counts taken from a single aliquot per time point. Time points correspond to those in *B*; cell samples for experiments in *D* and *E* were derived from the growth-profile experiment shown in *A*.

ribosome complex because a HigB H92Q mutant lacked mRNA cleavage activity but remained associated with the ribosome. Finally, the cleavage specificity of HigB on plasmid Rts1 coincided with the sequence (AAA, lysine) of either the most abundant or the second most abundant codon in its *Proteus* host.

EXPERIMENTAL PROCEDURES

Strains, Plasmids, and Reagents—The *E. coli* strains BL21(DE3) (F^- *omp*T *hsd*S_β(r_β-m_β) *dcm gal* (DE3) tonA) (Novagen) and BW25113 (*lacI*^{q} *rrnB*$_{T14}$ Δ*lac-Z*$_{WJ16}$ *hsdR514* Δ*araBAD*$_{AH33}$ Δ*rhaBAD*$_{LD78}$) were used for all protein expression and toxicity studies. *E. coli* K12 Mach1 T1 cells (Δ*rec*A1398 *end*A1 *ton*A Φ80Δ*lac*M15 Δ*lac*X74 *hsd*R($r_k^+m_k^+$); Invitrogen) were used for all cloning experiments. The *higBA* module was cloned from the Rts1 plasmid (a generous gift from Dr. Roger Woodgate, National Institutes of Health). The *E. coli* BW25113 strain with deleted *chpBI-BK*, *hipBA*, *mazEF*, *relBE*, *yefM-yoeB*, and *dinJ-yafQ* modules (BW25113 Δ6) was a generous gift from Qian Tan and Yoshi Yamaguchi of the M. Inouye laboratory. Plasmids used in this study include pBAD24 (23), pET28a (Novagen), and pBAD/*Myc*-HisA (Invitrogen). The *higBA* operon was PCR-amplified from the Rts1 vector with 5′ BamHI/HindIII 3′ ends and cloned into the corresponding sites of pET28a to create pET28a-*higBA*-$(His)_6$ with the His_6 tag fused onto *higB*. The *higB* ORF was PCR-amplified from the Rts1 vector with 5′ NdeI/Xho 3′ ends and cloned into the corresponding sites of pBAD24 to create pBAD24-*higB*. The *relE* ORF was PCR-amplified from BW25113 cells with 5′ NdeI/Xho 3′ ends and cloned into the corresponding sites of pBAD24 to create pBAD24-*relE*. The *higA* ORF was PCR-amplified from the Rts1 vector with 5′ BamHI/HindIII 3′ ends and cloned into the corresponding sites of pET28a to create pET28a-*higA*-$(His)_6$. The *higB* ORF was PCR-amplified from the Rts1 vector with 5′ Nco/HindIII 3′ ends, and an additional GC on the 5′ end to maintain frame was cloned into the corresponding sites of pBAD/*Myc*-HisA to create pBAD/*Myc*-HisA-*higB*-$(His)_6$. The *higB* ORF was PCR-amplified from the Rts1 vector with 5′ NdeI/Xho 3′ ends and a mutated H92Q amino acid and cloned into the corresponding sites of pBAD24 to create pBAD24-*higB*(H92Q). All bacterial liquid cultures were grown in M9 minimal media (M9) supplemented with either 0.2% glucose or 0.21% glycerol at 37 °C, unless otherwise noted. The working concentrations of ampicillin, kanamycin, and chloramphenicol were 100, 40, and 34 μg/ml, respectively. The accuracy of the DNA sequences of PCR products used for cloning was confirmed by automated DNA sequence analysis. Polyclonal antibodies used for Western analysis were produced in rabbits using the HigBA complex as antigen (Pocono Rabbit Farm and Laboratory, Canadensis, PA).

DNA, RNA, and Protein Synthesis in Vivo—[^{35}S]Methionine (24), [*methyl*-^{3}H]thymidine, and [*methyl*-^{3}H]uracil (22) incorporation studies were carried out as described previously.

Analysis of mRNA Levels in E. coli—Total RNA was extracted using the hot phenol method as described previously (25). The radiolabeled DNA fragments used for Northern analysis were derived from PCR products, including open reading frames of the *E. coli* genes *lpp* (major outer membrane lipoprotein), *ompA* (outer membrane porin protein A), *ompF* (outer mem-

brane porin protein F), *rpsA* (ribosomal protein subunit A), or *tufA* (EF-Tu). RNA levels were quantified with a phosphorimager, and all sample values were normalized to their respective control (*i.e.* the wild type uninduced values).

Ribosome Profile Analysis—Ribosomal extracts were prepared as described previously (14); equivalent amounts of total RNA from S30 extracts were layered onto each continuous sucrose gradient.

Primer Extension—Primer extension analysis was carried out as described previously (14). Primers used were as follows: *lpp*, 5′-TTACTTGCGGTATTTAGTAGCC-3′; *ompA3*, 5′-CCGCCAGCGAAGACCGGAGAAACGCCGG-3′; *ompA5*, 5′-TCAGAACCGATGCGGTCGGTGTAACCC-3′; *ompF*, 5′-AAACCAAGACGGGCATAGGTC-3′; *rpsA*, 5′-CGTCAACTTCGTCACCTACC-3′; and *tufA*, 5′-GAGAAGTGTTGATGGTGATACC-3′.

Recombinant HigA and HigB—The *higA*$(His)_6$-pET28a and *higB*$(His)_6$-pBAD/*Myc*-HisA constructs were transformed into BL21(DE3) and BW25113 cells, respectively, and induced with 1 mM isopropyl 1-thio-β-D-galactopyranoside (*higA*$(His)_6$-pET28a) or 0.2% arabinose (*higB*$(His)_6$-pBAD/*Myc*-HisA) for 6 h. Cells were disrupted using a French press; the protein extracts were applied to nickel-nitrilotriacetic acid resin (Qiagen), and the His_6-tagged proteins were purified as recommended by Qiagen. The protein content of each eluted fraction was visualized by 17.5% SDS-PAGE followed by Coomassie staining.

Determination of HigB(His)$_6$ Activity in Vitro—Prokaryotic cell-free protein synthesis was carried out with the *E. coli* T7 S30 extract system for circular DNA (Promega); the HigA only, HigB only, and HigB/HigA samples contained 2 μg of HigA$(His)_6$, 0.5 μg of HigB$(His)_6$, or 2 μg of HigA$(His)_6$ plus 0.5 μg of HigB$(His)_6$, respectively. The HigB/HigA samples were preincubated for 30 min at 4 °C prior to the addition of total RNA and the samples incubated for an additional 30 min at 37 °C.

Total cellular RNA was isolated from BW25113 cells as described above. 10 μg of total RNA was added to a reaction containing increasing amounts of pure recombinant HigB in 10 mM Tris, pH 7.8.

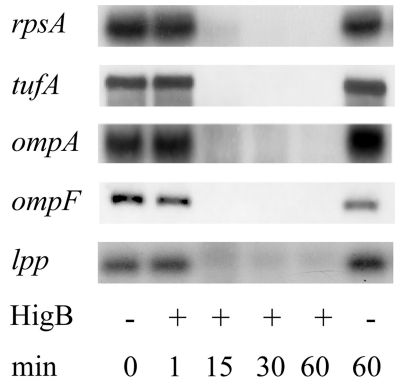

FIGURE 2. **Expression of HigB decreases steady state levels of several mRNAs *in vivo*.** RNA was extracted from HigB-expressing cells followed by Northern analysis. No visible degradation products were detected below the full-length mRNA in any of the +*HigB lanes*.

RESULTS

Expression of HigB Inhibits Translation—Although it has been reported that HigB inhibits protein synthesis through

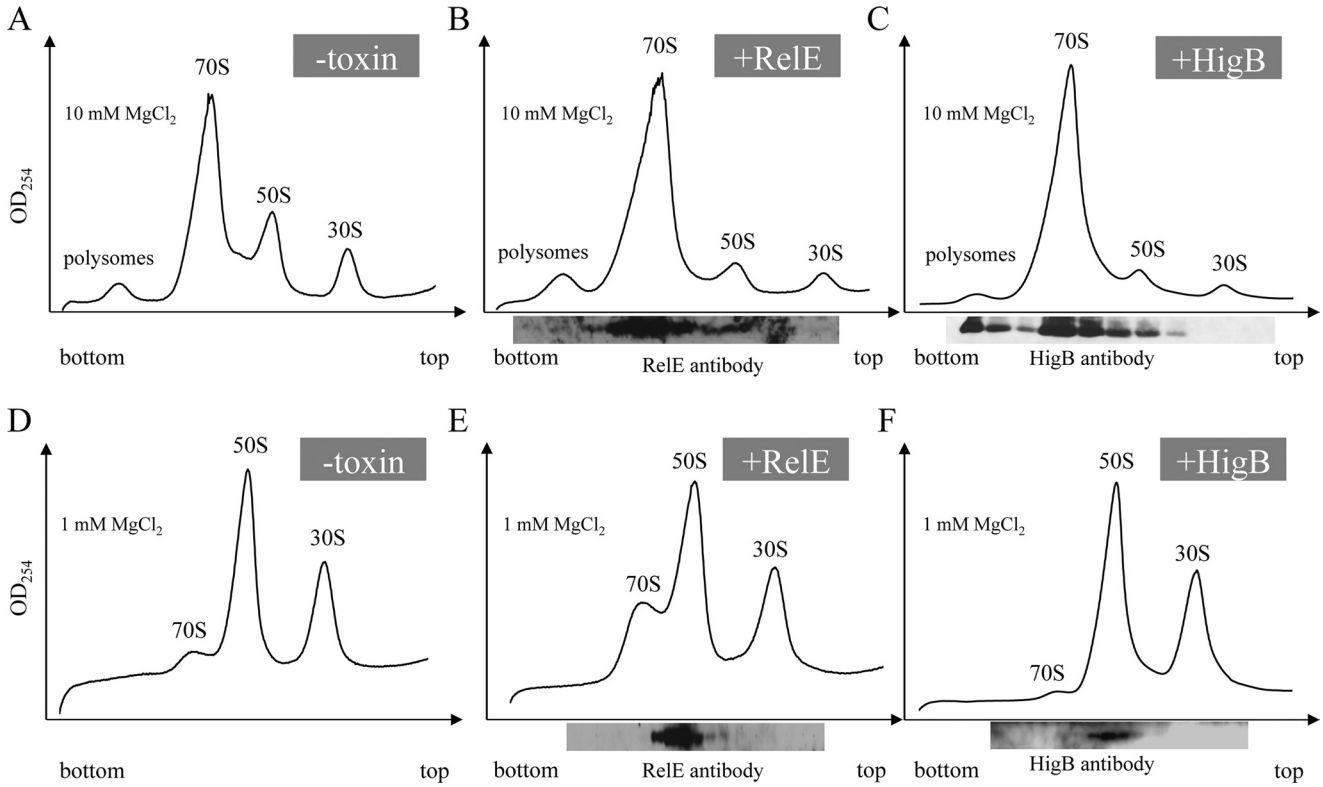

FIGURE 3. **HigB and RelE associate with ribosomes *in vivo*.** *A–C*, ribosomes prepared and fractionated in 10 mM Mg^{2+}; *D–F*, 1 mM Mg^{2+}. Ribosome profiles of wild type BW25113 cells (*A* and *D*), RelE (*B* and *E*), and HigB (*C* and *F*) are shown. Western blots (shown below fraction numbers tested) in *B, C, E,* and *F* were performed using antibody directed against either RelE or HigB. All 10 mM Mg^{2+} ribosome profiles were repeated three times.

translation-dependent mRNA cleavage (22), we characterized the enzymatic activity of HigB (92 amino acids, 10.7 kDa) from the Rts1 plasmid in more detail and compared its properties to family member RelE. We first expressed *relE* or *higB* in the arabinose-inducible pBAD24 plasmid. We found that the high toxicity of either RelE or HigB precluded the isolation of a stable strain containing either toxin gene in pBAD24 under noninducing conditions with glycerol as the carbon source. Therefore, in this study we used glucose under noninducing conditions and arabinose/glycerol for induction to minimize leaky toxin expression. As an additional precaution, all experiments were performed with strains that were recently transformed with the relevant toxin-expressing plasmid to preclude the accumulation of genomic suppressors of toxicity. To test whether induction using this unconventional method (glucose to arabinose/glycerol) was effective, we monitored growth after induction of *higB* or *relE* at mid-logarithmic phase. Expression of either *higB* (Fig. 1*A*) or *relE* (data not shown) resulted in growth arrest by 30 min. Interestingly, although both toxins arrested growth at approximately the same time, striking differences in [^{35}S]methionine incorporation were observed upon toxin induction (Fig. 1, *B–E*). RelE expression led to an extremely rapid shut down of translation (to ~5% of wild type within 5 min), whereas a more gradual decrease in protein synthesis was noted upon HigB expression; only at the 22-min time point did the effect of HigB remain constant (where translation levels dropped to 20% of wild type levels). This and previously published data (22) are consistent with a model whereby RelE and HigB cause growth arrest by blocking translation. In fact, *in vivo* incorporation of radiolabeled precursors of DNA or RNA revealed that expression of HigB did not lead to significant defects in DNA replication or RNA transcription (supplemental Fig. 1).

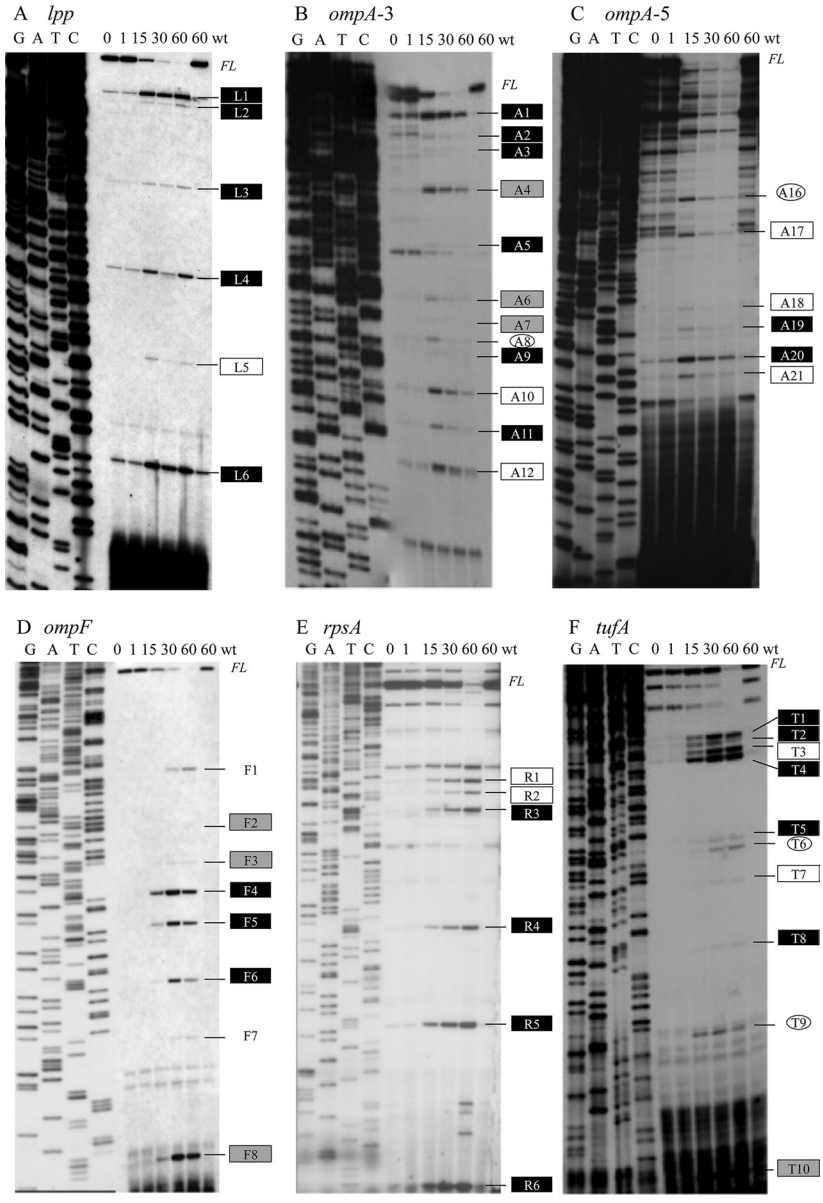

G

lpp	Cut site	Major /minor	*ompA*	Cut site	Major/ minor
5' ATG AA GCT ACT 3'	L1	M	5' ACT AA AAG ACA 3'	A1	M
5' GCT ACT AA CTG GTA 3'	L2	m	5' GCT CCG AA GAT AAC 3'	A2	m
5' AAC GCT AA ATC GAT 3'	L3	m	5' GGT GCT AA CTG GGC 3'	A3	m
5' AAC GCT AA GTT GAC 3'	L4	M	5' CAT GA AA C CAA CTG 3'	A4	M
5' AAC GC A TG CGT TCC 3'	L5	m	5' GGC TTT G AA ATG GGT 3'	A5	m
5' GCT GCT AAA GAT GCA 3'	L6	M	5' CCG TAC AAA GGC AGC 3'	A6	m
ompF			5' AGC GTT G AA AAC GTT 3'	A7	m
5' AAT ATT CTT GCA GTG 3'	F1	m	5' AAC GGT GC A TAC AAA 3'	A8	m
5' GGT ACT GC A AAC GCT 3'	F2	m	5' GCA TAC AA GCT CAG 3'	A9	m
5' GCT GCA GAA ATC TAT 3'	F3	m	5' GGC GTT C AA CTG ACC 3'	A10	M
5' TAT AAC AA GAT GGC 3'	F4	M	5' ACC GCT AA CTG GGT 3'	A11	M
5' GGC AAC AA GTA GAT 3'	F5	M	5' GGT TAC CC A ATC ACT 3'	A12	M
5' TAC GGT AA GCT GTT 3'	F6	M	5' GAC ACT AA TCC AAC 3'	A13	M
5' GGT CTG CAT TAT TTT 3'	F7	m	5' TAT GGT AA AAC CAC 3'	A14	M
5' AAC GGT GAA AAC AGT 3'	F8	M	5' ACT CCT GA A ATC GCT 3'	A15	M
rpsA			5' GCA GCT CC A GTA GTT 3'	A16	M
5' TTT GCT CA CTC TTT 3'	R1	M	5' GCA CCG GA AA GTA CAG 3'	A17	M
5' CTC TTT CA AAG TCC 3'	R2	M	5' CTG TCC AA C TTC AAC 3'	A18	m
5' TCC TTA AA GAA ATC 3'	R3	M	5' TTC AAC AA GCA ACC 3'	A19	m
5' ATC GAC AA GAC GTA 3'	R4	M	5' ACC CTG AA CCG GAA 3'	A20	M
5' GGT CTG AA TCT GAG 3'	R5	M	5' AAA CCG GA AA GGT CAG 3'	A21	m
5' CAG TTC AA AAC GCC 3'	R6	M	5' GAT CCG AA GAC GGT 3'	A22	M
tufA			5' ATC TCC AA GGT ATC 3'	A23	m
5' GTG TCT AA GAA AAA 3'	T1	M	5' ATG GGC GA TCC AAC 3'	A24	m
5' AAA GAA AA TTT GAA 3'	T2	m	5' AAC GTG AAA CAG CGT 3'	A25	M
5' AAA TTT GA CGT ACA 3'	T3	M			
5' CGT ACA AAA CCG CAC 3'	T4	M			
5' CAC GGT AA ACT ACT 3'	T5	m			
5' AAA ACT C CT CTG ACC 3'	T6	m			
5' ACC GCT GC A TC ACC 3'	T7	m			
5' CTG GCT AA ACC TAC 3'	T8	m			
5' GCT CGT GC T TTC GAC 3'	T9	m			
5' CCG GAA GA A AAA GCT 3'	T10	M			

H

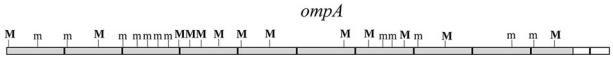

Expression of HigB Leads to Rapid and Extensive Degradation of Several mRNAs in Vivo—HigB or RelE expression results in degradation of *lpp* mRNA only when the start codon is intact (11, 22). To determine whether HigB affects the stability of several transcripts, we performed Northern analysis for five *E. coli* mRNAs: *lpp*, *ompA*, *ompF*, *rpsA*, and *tufA* (Fig. 2). Although no degradation was detectable immediately after (1 min) induction of HigB expression, degradation was extensive after 15 min; after 60 min, degradation of all five transcripts were complete or nearly complete. In comparison, the steady state levels of the respective control mRNAs (cells harboring the plasmid but not expressing HigB) were stable. No visible degradation products were detected below the full-length mRNA in any of the +HigB lanes.

To ensure that the mRNA degradation we observed upon HigB induction was not due to activation of other TA toxins resulting from the inherent stress of HigB expression, we expressed HigB in an *E. coli* strain ("Δ6") in which each of the six known chromosomal TA modules has been deleted (*mazEF, relBE, chpBI-BK, hipBA, yefM-yoeB,* and *dinJ-yafQ*). The levels of full-length *lpp*, *ompA*, and *rpsA* transcripts were compared in Δ6 and BW25113 cells before and after induction of the toxin. We found no difference in the steady state levels of each of the three mRNAs in the two strains after HigB induction (supplemental Fig. 2). The same experiments were also performed with RelE, and no difference was observed (supplemental Fig. 2). Therefore, HigB or RelE expression appears to lead to global degradation of cellular mRNA *in vivo,* and this effect does not enlist the action of other toxins.

HigB Associates with the Ribosome through the 50 S Ribosomal Subunit—Mutagenesis of the *lpp* AUG start codon to AAG prevents *lpp* mRNA degradation *in vivo*, revealing that the action of HigB is translation-dependent (as is family member RelE) (22). These data suggest that HigB acts through interaction with the ribosome. Therefore, we analyzed ribosome profiles from cells overexpressing HigB for 60 min (when cells were completely growth-arrested and cellular mRNA degradation in Fig. 2 was maximal) to assess whether toxin expression altered the profile (Fig. 3, compare *A* and *C*). We also used Western analysis of fractions spanning the sucrose gradient to determine whether we were able to identify an association of HigB with the ribosome (Fig. 3*C*). We did not observe additional peaks or substantial changes in polysome, 70 S, 50 S, or 30 S sedimentation. However, HigB led to the increase in the relative abundance the 70 S monosome because we reproducibly noted a higher relative ratio of 70 S monosome compared with both 50 S/30 S ribosomal subunit peaks upon HigB induction (compare Fig. 3, *A* and *C*). In extracts/gradients containing the standard 10 mM Mg^{2+}, HigB associated primarily with 70 S monosomes, but it was also detected with the 50 S ribosomal subunit and polysomes. However, HigB was not associated with the 30 S ribosomal subunit (Fig. 3*C*). In addition, buffer conditions favoring dissociation of the 70 S ribosome to its component subunits (1 mM Mg^{2+}) confirmed that HigB associates with only the 50 S ribosomal subunit and not the 30 S. Thus, HigB associates with the ribosome through the 50 S ribosomal subunit *in vivo* (Fig. 3*F*).

Other members of the RelE family, YafQ (14) and YoeB (15), associate with ribosomes through the 50 S subunit. Therefore, we analyzed the ribosome profile for RelE association with these fractions just as we had for HigB to determine whether this is a common property of RelE family members (Fig. 3, compare *A* and *B*). The ribosome profile for RelE was similar to that for HigB, with a higher relative ratio of 70 S to 50/30 S peaks, and as with the other three RelE family members tested, it interacted with the ribosome through the 50 S subunit (Fig. 3, *B* and *E*).

HigB Facilitates Ribosome-dependent Cleavage of mRNA at A-rich Sequences—Because HigB associated with the ribosome and facilitated extensive mRNA cleavage, we determined the sequence specificity and frame dependence of its cleavage activity and recognition sequence. We isolated total RNA from HigB induced and uninduced cells and performed primer extension analysis on the five mRNAs (*lpp*, *ompA*, *ompF*, *rpsA,* and *tufA*) that were degraded upon HigB expression in Fig. 2. We initially used a primer ~150 nucleotides downstream of the 5′ end of the translation start site for each mRNA and then performed additional primer extension experiments to enable nearly complete coverage of *lpp* (237 bp) and *ompA* (1041 bp; Fig. 4, *A–F*). In total, we detected 55 HigB-specific cleavage products among all mRNAs (Fig. 4*G*). Of these, 30 were major sites representing relatively abundant cleavage products, and 25 were minor sites whose intensities were approximately ≤25% that of the major sites. Note that HigB is a very potent toxin; even though we used glucose prior to induction to minimize leaky expression of the toxin gene, some HigB-mediated cleavage was detected even in the uninduced time points. Therefore, we were careful to choose only those primer extension products that increased with induction time relative to the uninduced control.

Analysis of the sequence and location of all cleavage sites revealed several features of HigB-mediated cleavage as follows. 1) 5′-AAA-3′ is the primary recognition consensus sequence (highlighted in *black* and in *gray* in Fig. 4*G*). We found that HigB cleaved 100% of the AAA sequences covered in our primer extension analyses. The regions we tested contained 38 AAA sites, and we documented cut sites for all of them (23 major and 15 minor).

FIGURE 4. **HigB-mediated sequence-specific, frame-independent mRNA cleavage.** Primer extension analysis of the following: *A, lpp*; *B, ompA-3*; *C, ompA-5*; *D, ompF*; *E, rpsA*; and *F, tufA* mRNAs extracted from cells expressing HigB. Exact cleavage positions of mRNAs identified near the top of the gel were determined with closer primers (data not shown); *FL,* full-length products; *wt,* wild type. Labeled cut sites correspond to those reported in *G*. Note that some HigB-mediated cleavage was detected even in the uninduced time points; only those products that increased with induction time relative to the uninduced control were highlighted. *G,* summary of HigB cleavage sites (spacing denotes translational frame) as follows: in-frame AAAs (*black rectangle*); out-of frame AAAs (*gray rectangle*); AA (*open rectangle*); and single A (*open oval*). The two unmarked sites for *ompF* correspond to putative RNase E sites. *H,* location of major and minor cleavage products for the *ompA* mRNA. Cleavage sites in the region corresponding to the *white box* at 3′ end could not be detected; this region was where the terminal primer annealed. The drawing is to scale, with each *black line* demarcating 100 nucleotides.

2) HigB targets both in-frame and out-of-frame AAA or AAA-containing sequences for cleavage (compare *black versus gray* highlighted sequences in Fig. 4*G*).

3) HigB also cleaved stretches of four or more A-rich sequences; moreover, HigB cleaved within the first three AAAs in A_4 or A_5 stretches in six of the seven examples we uncovered.

4) The location of the cleavage site in the AAA site (or the first three As in A_4 or A_5 sequences) was not fixed but instead exhibited a preference for cleavage after the second A, *i.e.* 5′-AA ↓ A-3′. More specifically, 45% were 5′-AA ↓ A-3′, 29% 5′-A ↓ AA-3′, 13% 5′ ↓ AAA-3′, and 13% 5′-AAA ↓ -3′.

5) HigB cleaves throughout the length of the mRNA (see illustration for *ompA*, Fig. 4*H*) with no apparent pattern for major and minor site distribution.

6) HigB also recognized AA sequences with much lower efficiency (20% of the 55 cut sites; *open rectangles* in Fig. 4*G*) and occasionally cut at single A sequences (4/55, 7%; *open ovals*, Fig. 4*G*).

7) Two of the 55 HigB-specific cleavage sites (both in *ompF*) did not cut at an A residue. Instead, the sequences 5′-AAUAUU ↓ CUUGC-3′ (F1) and 5′-GCAU ↓ UAUU-UUU-3′ (F7) have similarity to RNase E consensus sites (26, 27). RNase E is a single strand-specific endoribonuclease required for rapid mRNA decay and accurate RNA processing in *E. coli*. Therefore, HigB cleavage of *ompF* and other mRNAs may be assisted by RNase E and the degradasome (28).

8) We did not detect cleavage sites in the 5′-untranslated regions upstream of the five mRNAs, corroborating our data demonstrating HigB ribosome association and earlier studies demonstrating that *lpp* mRNA must have an intact start Met codon for HigB-mediated degradation (11).

HigB Does Not Cleave RNA in Vitro—To better characterize the mechanism of HigB-mediated mRNA cleavage, we assessed whether HigB possessed endoribonuclease activity *in vitro*. As a first step, we purified recombinant HigB toxin and confirmed that it was active using a coupled *in vitro* transcription/translation assay with or without the addition of HigB toxin or with both HigB toxin/HigA antitoxin. Recombinant HigB inhibited *in vitro* translation, and the effects of HigB were reversed by addition of the antitoxin HigA (Fig. 5*A*). Therefore, these recombinant proteins were active after purification.

We next tested if the same HigB preparation was able to cleave total RNA purified from *E. coli* K12. No cleavage was detected in either mRNA or rRNA after a 30-min incubation of total RNA with increasing concentrations of HigB. There was also no effect on the RNA when the HigA antitoxin was added to the HigB (Fig. 5*B* and data not shown). When the incubation time was increased to 6 h, we also did not detect RNA cleavage. These results suggest that the HigB-mediated *in vivo* cleavage activity is dependent upon interaction with the ribosome.

HigB(H92Q) Abolishes Toxicity and mRNA Cleavage but Not Ribosome Binding—X-ray crystal structures of RelE, YoeB, and accompanying mutagenesis studies (29, 30) implicated a highly conserved histidine near their carboxyl termini as important for their toxicity. However, subsequent studies on YoeB demonstrated that mutagenesis of this conserved histidine (H83Q) did not lead to a loss in toxicity or a reduction in its primary function as an inhibitor of translation initiation (15). In contrast,

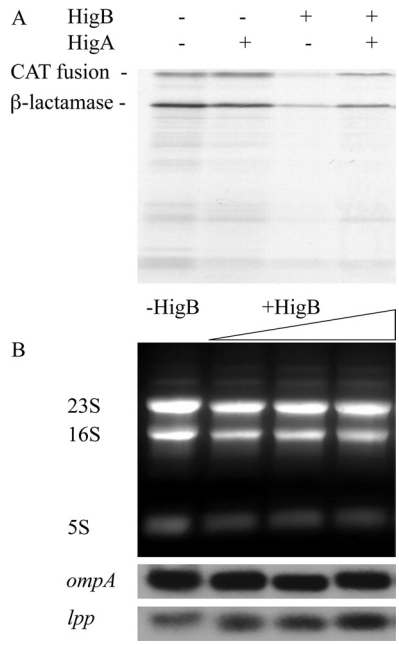

FIGURE 5. **HigB inhibits translation but does not degrade mRNA *in vitro*.** *A,* recombinant HigB inhibits coupled *in vitro* transcription/translation (*3rd lane*); HigA can rescue the inhibition and reconstitute translation (*4th lane*) to normal levels (as shown in *1st lane*); the product of the chloramphenicol acetyltransferase (*CAT*) fusion template (39 kDa) includes one of the two major reaction products, and the other β-lactamase (28 kDa) product is present at high levels in T7 S30 extracts because of transcription from the T7 promoter upstream of the chloramphenicol acetyltransferase fusion that reads through into the ampicillin resistance gene. *B,* HigB does not cleave rRNA or mRNA *in vitro*. *1st lane,* 10 μg of total RNA; *2nd*, *3rd*, and *4th lanes*, increasing amounts of purified HigB$(His)_6$ were added to 10 μg of total RNA.

mutagenesis of the corresponding residue in YafQ (31) (H87Q) abolished YafQ toxicity and endoribonuclease activity *in vivo* (14).

Because HigB is in the RelE family, we aligned all family members and noted that HigB from the Rts1 plasmid and *E. coli* CFT073 also contained a highly conserved histidine (His-92 for Rts1 and His-90 for *E. coli* CFT073) at the carboxyl-terminal end of their primary sequences. Because active HigB did not exhibit detectable ribonuclease activity *in vitro*, it may mediate mRNA cleavage only upon association with the ribosome *in vivo*. Alternatively, as suggested for RelE (13), there was a formal possibility that the HigB mRNA cleavage activity we documented *in vivo* was because of an enhancement of the intrinsic mRNA cleavage activity of the ribosome (32). Therefore, to differentiate between these possible modes of action, we created an H92Q mutant in Rts1 HigB and examined the growth rate of the mutant strain upon induction of HigB(H92Q). Unlike wild type HigB, induction of HigB(H92Q) no longer resulted in growth arrest (Fig. 6*A*), indicating that His-92 is essential for HigB-mediated toxicity. We then determined the effect of HigB(H92Q) expression on the steady state levels of *ompA* and *lpp* transcripts and found no difference compared with the wild type control (cells harboring the plasmid but not expressing HigB(H92Q)) (Fig. 6*B*), *i.e.* mRNA was no longer degraded in cells expressing the HigB(H92Q) mutant. Finally, ribosome profile analysis revealed that the mutant HigB(H92Q) toxin retained its ability to associate with the ribosome (Fig. 6, *C* and *D*). Therefore, the endoribonuclease activity of the HigB-ribo-

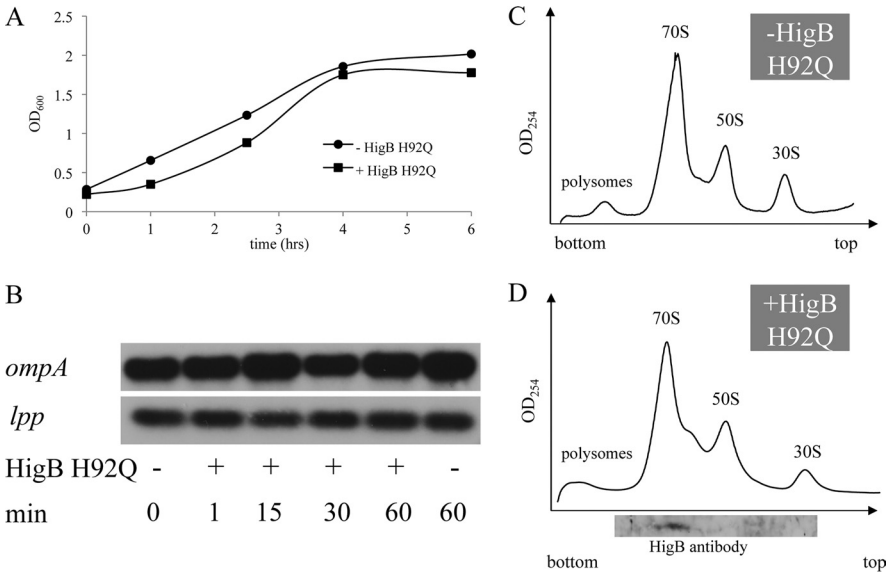

FIGURE 6. **HigB(H92Q) expression results in loss of toxicity (*A*) and mRNA cleavage (*B*) but not ribosome binding (*C* and *D*).**

some complex appears to be conferred by HigB, and this activity requires His-92.

DISCUSSION

The HigBA TA system is essential for plasmid maintenance of the kanamycin-resistant Rts1 plasmid (19). Notably, although the *E. coli* K12 chromosome contains only a *higA* homolog, its pathogenic relatives *E. coli* CFT073 and *E. coli* O157:H7 appear to possess one or more copies of the entire module (20). In fact, the chromosomes of many pathogenic bacteria contain one or more *higBA* modules; this is also true for many bacteria with slow growth rates or characteristically long dormant periods (20). Toward a better understanding of how this toxin imparts mRNA degradation, a concomitant block in protein synthesis, and growth arrest (21, 22), we determined that the ribosome-HigB complex targets actively translated mRNA for cleavage at A-rich sequences. HigB cuts 100% of in-frame and out-of-frame AAA sequences in the coding regions of mRNAs (including the first three AAAs of stretches of 4 or more As). HigB also cuts AA sequences but with much lower efficiency (20%), and only occasionally cuts at single As.

The conjugative Rts1 plasmid was obtained from a clinical isolate of *Proteus vulgaris* (33). Analysis of the available codon usage data for *P. vulgaris* (323 coding regions, the majority comprising genes of the Rts1 plasmid) revealed that HigB cleaves at a target sequence that corresponds to the most common codon, AAA (lysine 41.0/1000 codons). The second most common codon, GAA (glutamic acid 38.3/1000 codons), also contains an AA HigB cleavage site.

However, Rts1 can also replicate in *Proteus mirabilis* (34), which causes the majority of *Proteus* urinary tract infections. Analysis of the codon usage data for the complete genome of *P. mirabilis* revealed that HigB cleaves at a target sequence that corresponds to the second most common codon, AAA, encoding lysine (46.5/1000 codons) for the *P. mirabilis* genome (leucine is the most used codon at 48.6/1000 codons). Although leucine is also the most common codon in *E. coli* K12 (52.82/1000 codons), AAA is represented at lower frequency (33.62/1000 codons) than in *P. mirabilis.*

Although the complete genome sequence of *P. vulgaris* has not been reported, it is AT-rich (61%) (35) as is the genome of *P. mirabilis* (also 61% AT) (36). For comparison, the *E. coli* K12 genome has a lower AT content (49%) (37). Curiously, the sequenced *P. mirabilis* strain contains a plasmid distinct from Rts1 that is designated pHI4320. Not only is AAA lysine the most common codon in this plasmid, it is almost twice as abundant compared with its host genome (76.3/1000 codons). Perhaps Rts1 has adapted to have a selective advantage when a *Proteus* strain contains both Rts1 and pHI4320 plasmids such that any free HigB would selectively degrade mRNA of its competitor plasmid. More specifically, if only Rts1 is cured, not only would the remaining stable HigB toxin degrade host mRNA, it should also degrade the competitor plasmid even more efficiently, ensuring an advantage for retention of Rts1 over pHI4320. In summary, these data suggest that the HigB cleavage site exploits the Achilles' heel of its host (*i.e.* A-rich sequences both in-frame or out-of-frame) to maximize its potency when conditions lead to plasmid loss and warrant post-segregational killing.

Studies in *E. coli* K12 have also linked the presence of an AAA codon at +2 to high translation initiation efficiency (38, 39). AAA is also the most common codon at +2, represented in ~10% of all *E. coli* K12 mRNAs containing AUG or GUG start codons (39). Purine-rich sequences, especially adenine-rich ones, are correlated with single strand regions in 16 S rRNA (40). Thus the higher translational efficiency when A-rich sequences are found 3′ of the translation start site may be due to the absence of mRNA secondary structure. The high AT content of the *P. vulgaris* and *P. mirabilis* genomes suggests that these strains may also contain a higher than average number of AAA codons early in the mRNA. In fact, we surveyed 100 random open reading frames from the *P. mirabilis* genome and found an even higher percentage (17%) of AAAs at +2 than *E. coli* K12. Therefore, HigB acts on multiple levels of its characteristically AT-rich host cells. First, it targets one of the most abundant codons (AAA) of its host cell for cleavage. Second, it also cleaves all AAA-containing sequences independent of frame. Third, it cleaves specific AAs (~20% of the total) and occasionally cleaves specific single As. Fourth, targeting highly expressed mRNAs containing AAA at +2 may enhance the potency of HigB. In concert, this multitiered mechanism ensures rapid and efficient post-segregational killing of hosts that lose the Rts1 plasmid.

The analysis of the molecular mechanism of HigB completes the characterization of all four representative members of the

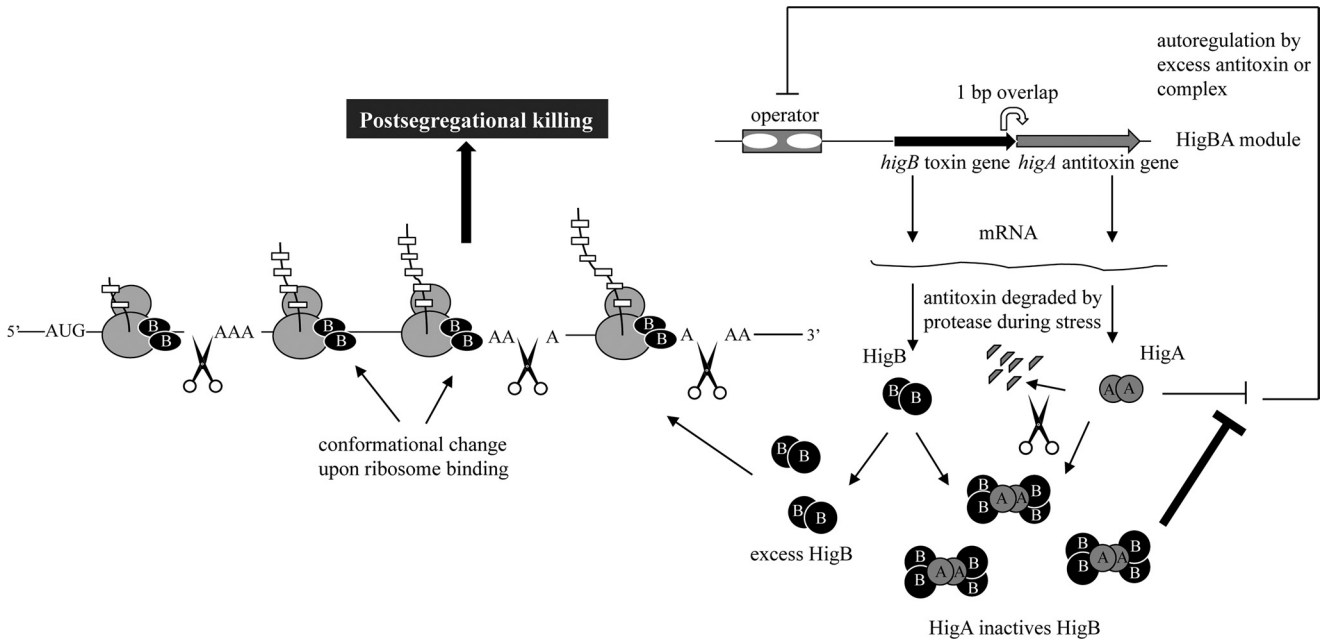

FIGURE 7. **Features of HigB-HigA function in *E. coli*.** Toxin and antitoxin mRNAs are synthesized from an autoregulated operon, and the open reading frame of the toxin overlaps the antitoxin gene by 1 bp (19). HigBA is distinct from other TA systems because the toxin gene precedes the antitoxin. Both HigB/HigA and HigA autoregulate the operon by binding to the operator consisting of two subsites (subsite one includes the palindrome 5′-TATTGCACATCGTGTAATA-3′, and subsite two includes the palindrome 5′-GTATTACACACCATGTAATAC-3′) (18). HigA/HigB-mediated repression is 4-fold higher than that by HigB alone (18). HigB associates with actively translating 70 S ribosomes through the 50 S ribosomal subunit. The interaction of HigB with ribosomes appears to cause an allosteric change in HigB that activates its site-specific endoribonuclease activity (represented by a change in HigB shape). HigB then travels with the translating ribosome and cleaves the mRNA when it reaches the first major or minor A-rich consensus sequence. The tmRNA system cannot accommodate the extensive mRNA degradation, resulting in slower ribosome recycling (shown by HigB disomes). This unchecked block in translation elongation leads to bacterial cell death (*i.e.* post-segregational killing for cells that have lost the Rts1 plasmid).

RelE family as follows: RelE, YafQ, and YoeB from *E. coli* K12 and HigB from plasmid Rts1. All four family members act through the association with the 50 S ribosomal subunit of the 70 S ribosome. However, each imparts toxicity through distinct mechanisms. YafQ possesses ribonuclease activity *in vitro* and *in vivo* but acquires its frame-dependent, sequence-specific activity only upon association with the ribosome *in vivo* (14). HigB only acquires ribonuclease activity upon association with the ribosome and cleaves its recognition sequences on translating mRNAs both in- and out-of-frame. In contrast, neither RelE nor YoeB alone exhibits endoribonuclease activity *in vitro* (13, 15), and mRNA cleavage is only secondary for YoeB-mediated inhibition of translation initiation *in vivo* (15). The *in vivo* mRNA cleavage activity associated with RelE has been linked to the endonucleolytic activity of the ribosome (32).

We propose the following model of HigB-mediated post-segregational killing (Fig. 7). Because we documented HigB-mediated cleavage throughout the length of mRNAs (see Fig. 4*H*), HigB appears to associate with actively translating 70 S ribosomes through the 50 S ribosomal subunit. HigB may also associate with the 50 S ribosomal subunit as it assembles into a 70 S monosome based on the following. 1) It can cleave mRNA very early, at the second codon of *lpp* (Fig. 4*G*); and 2) it was also detected in the 50 S fraction in 10 mM Mg^{2+} profiles (Fig. 3*C*). The interaction of HigB with ribosomes appears to cause an allosteric change in HigB that activates its site-specific endoribonuclease activity. HigB then travels with the translating ribosome and cleaves the mRNA when it reaches the first major or minor A-rich consensus sequence; however, our data do not enable us to distinguish if HigB cleaves at the first consensus site it reaches or subsequent ones. This extensive cleavage results in rapid mRNA degradation and inhibition of translation elongation. As a consequence, the tmRNA system for rescuing stalled ribosomes is overwhelmed, resulting in slower ribosome recycling evidenced by the reproducibly higher 70 S peak (that we propose represents stalled ribosomes) as well as the presence of HigB in the disome fraction in Fig. 3*C* (because ribosomes without bound HigB will not be able to continue translating past the stalled ribosome at the HigB cut site). The high AT content of the *Proteus* host genomes are remarkably complementary to the overall mechanism of HigB action and may portend the existence of a similar adaptation for chromosomal HigB counterparts.

Acknowledgments—We thank Roger Woodgate for providing the Rts1 plasmid and Yoshi Yamaguchi for the construction and use of the BW25113 Δ6 strain. We also thank the members of the laboratory for manuscript proofreading; Yonglong Zhang for the RelBE polyclonal antibody; Koichi Inoue for guidance; and Masayori Inouye for extensive advice and expertise.

REFERENCES

1. Gerdes, K., Christensen, S. K., and Løbner-Olesen, A. (2005) *Nat. Rev. Microbiol.* **3,** 371–382
2. Engelberg-Kulka, H., and Glaser, G. (1999) *Annu. Rev. Microbiol.* **53,** 43–70
3. Amitai, S., Yassin, Y., and Engelberg-Kulka, H. (2004) *J. Bacteriol.* **186,** 8295–8300

4. Engelberg-Kulka, H., Hazan, R., and Amitai, S. (2005) *J. Cell Sci.* **118,** 4327–4332
5. Pedersen, K., Christensen, S. K., and Gerdes, K. (2002) *Mol. Microbiol.* **45,** 501–510
6. Christensen, S. K., Pedersen, K., Hansen, F. G., and Gerdes, K. (2003) *J. Mol. Biol.* **332,** 809–819
7. Muñoz-Gómez, A. J., Santos-Sierra, S., Berzal-Herranz, A., Lemonnier, M., and Díaz-Orejas, R. (2004) *FEBS Lett.* **567,** 316–320
8. Zhang, Y., Zhang, J., Hara, H., Kato, I., and Inouye, M. (2005) *J. Biol. Chem.* **280,** 3143–3150
9. Zhang, Y., Zhang, J., Hoeflich, K. P., Ikura, M., Qing, G., and Inouye, M. (2003) *Mol. Cell* **12,** 913–923
10. Zhang, Y., Zhu, L., Zhang, J., and Inouye, M. (2005) *J. Biol. Chem.* **280,** 26080–26088
11. Christensen, S. K., and Gerdes, K. (2003) *Mol. Microbiol.* **48,** 1389–1400
12. Christensen, S. K., Mikkelsen, M., Pedersen, K., and Gerdes, K. (2001) *Proc. Natl. Acad. Sci. U.S.A.* **98,** 14328–14333
13. Pedersen, K., Zavialov, A. V., Pavlov, M. Y., Elf, J., Gerdes, K., and Ehrenberg, M. (2003) *Cell* **112,** 131–140
14. Prysak, M. H., Mozdzierz, C. J., Cook, A. M., Zhu, L., Zhang, Y., Inouye, M., and Woychik, N. A. (2009) *Mol. Microbiol.* **71,** 1071–1087
15. Zhang, Y., and Inouye, M. (2009) *J. Biol. Chem.* **284,** 6627–6638
16. Correia, F. F., D'Onofrio, A., Rejtar, T., Li, L., Karger, B. L., Makarova, K., Koonin, E. V., and Lewis, K. (2006) *J. Bacteriol.* **188,** 8360–8367
17. Schumacher, M. A., Piro, K. M., Xu, W., Hansen, S., Lewis, K., and Brennan, R. G. (2009) *Science* **323,** 396–401
18. Tian, Q. B., Hayashi, T., Murata, T., and Terawaki, Y. (1996) *Biochem. Biophys. Res. Commun.* **225,** 679–684
19. Tian, Q. B., Ohnishi, M., Tabuchi, A., and Terawaki, Y. (1996) *Biochem. Biophys. Res. Commun.* **220,** 280–284
20. Pandey, D. P., and Gerdes, K. (2005) *Nucleic Acids Res.* **33,** 966–976
21. Budde, P. P., Davis, B. M., Yuan, J., and Waldor, M. K. (2007) *J. Bacteriol.* **189,** 491–500
22. Christensen-Dalsgaard, M., and Gerdes, K. (2006) *Mol. Microbiol.* **62,** 397–411
23. Guzman, L. M., Belin, D., Carson, M. J., and Beckwith, J. (1995) *J. Bacteriol.* **177,** 4121–4130
24. Hirashima, A., and Inouye, M. (1973) *Nature* **242,** 405–407
25. Sarmientos, P., Sylvester, J. E., Contente, S., and Cashel, M. (1983) *Cell* **32,** 1337–1346
26. Ehretsmann, C. P., Carpousis, A. J., and Krisch, H. M. (1992) *Genes Dev.* **6,** 149–159
27. Redko, Y., Tock, M. R., Adams, C. J., Kaberdin, V. R., Grasby, J. A., and McDowall, K. J. (2003) *J. Biol. Chem.* **278,** 44001–44008
28. Carpousis, A. J. (2007) *Annu. Rev. Microbiol.* **61,** 71–87
29. Kamada, K., and Hanaoka, F. (2005) *Mol. Cell* **19,** 497–509
30. Takagi, H., Kakuta, Y., Okada, T., Yao, M., Tanaka, I., and Kimura, M. (2005) *Nat. Struct. Mol. Biol.* **12,** 327–331
31. Motiejūnaite, R., Armalyte, J., Markuckas, A., and Suziedeliene, E. (2007) *FEMS Microbiol. Lett.* **268,** 112–119
32. Hayes, C. S., and Sauer, R. T. (2003) *Mol. Cell* **12,** 903–911
33. Terawaki, Y., Takayasu, H., and Akiba, T. (1967) *J. Bacteriol.* **94,** 687–690
34. Terawaki, Y., and Rownd, R. (1972) *J. Bacteriol.* **109,** 492–498
35. Falkow, S., Ryman, I. R., and Washington, O. (1962) *J. Bacteriol.* **83,** 1318–1321
36. Pearson, M. M., Sebaihia, M., Churcher, C., Quail, M. A., Seshasayee, A. S., Luscombe, N. M., Abdellah, Z., Arrosmith, C., Atkin, B., Chillingworth, T., Hauser, H., Jagels, K., Moule, S., Mungall, K., Norbertczak, H., Rabbinowitsch, E., Walker, D., Whithead, S., Thomson, N. R., Rather, P. N., Parkhill, J., and Mobley, H. L. (2008) *J. Bacteriol.* **190,** 4027–4037
37. Blattner, F. R., Plunkett, G., 3rd, Bloch, C. A., Perna, N. T., Burland, V., Riley, M., Collado-Vides, J., Glasner, J. D., Rode, C. K., Mayhew, G. F., Gregor, J., Davis, N. W., Kirkpatrick, H. A., Goeden, M. A., Rose, D. J., Mau, B., and Shao, Y. (1997) *Science* **277,** 1453–1474
38. Brock, J. E., Paz, R. L., Cottle, P., and Janssen, G. R. (2007) *J. Bacteriol.* **189,** 501–510
39. Stenström, C. M., Jin, H., Major, L. L., Tate, W. P., and Isaksson, L. A. (2001) *Gene* **263,** 273–284
40. Wang, H. C., and Hickey, D. A. (2002) *Nucleic Acids Res.* **30,** 2501–2507